ICAST2014#098

Structural Analysis of an Unconventional Hybrid Control Surface of a Morphing Wing

Pınar ARSLAN[1], Uğur KALKAN[2], Harun TIRAŞ[3], İlhan Ozan TUNÇÖZ[4], Yosheph YANG[5], Ercan GÜRSES[6], Melin ŞAHİN[7], Serkan ÖZGEN[8], Yavuz YAMAN[9]

Department of Aerospace Engineering, Middle East Technical University, Ankara, Turkey

Abstract

In this study, design and analysis of a new unconventional hybrid trailing edge control surface of an unmanned aerial vehicle (UAV) wing is presented. The hybrid trailing edge control surface is composed of a compliant material and a composite material and designed by using CATIA® V5-6R2012 package program. The stiffness difference between compliant and composite parts provides the deflection of control surface and an effective camber. The required number and the location of servo motors needed to deflect control surface effectively were compared by considering the desired shape of the control surface, weight and torque optimization. The servo motor forces that gave the desired shape of the control surface were determined in-Vacuo condition by using ANSYS®v14.0 Workbench package program to perform finite element analysis (FEA). Then, the structural analysis of the control surface is performed under the aerodynamic loads which were taken from a similar study. [1] Finally, in order to demonstrate that the design is realizable, it is shown that the servo motors can fit within the control surface.

[1] Pınar Arslan, pinar.arslan@metu.edu.tr
[2] Uğur Kalkan, ugur.kalkan@metu.edu.tr
[3] Harun Tıraş, tiras.harun@metu.edu.tr
[4] İlhan Ozan Tunçöz, ozan.tuncoz@metu.edu.tr
[5] Yosheph Yang, yosheph.yang@metu.edu.tr
[6] Ercan Gürses, gurses@metu.edu.tr
[7] Melin Şahin, msahin@metu.edu.tr
[8] Serkan Özgen, sozgen@ae.metu.edu.tr
[9] Yavuz Yaman, yyaman@metu.edu.tr

1. INTRODUCTION

Unconventional control surfaces are often heavier than the conventional ones, due to the complexity of unconventional ones. In order to reduce the required actuation forces and the weight of the control surface, authors propose a hybrid control surface. In this study, a hybrid trailing edge control surface was designed and developed for landing phase of the flight of an unmanned aerial vehicle (UAV), which is being developed within the scope of CHANGE (*Combined morpHing Assessment software usiNG flight Envelope data and mission based morphing prototype wing development*) Project financed under the 7th Framework Programme of the European Comission. [2]

In this study, the trailing edge control surface was initially attached to the baseline wing provided by a partner of the CHANGE project, Aircraft Research Association (ARA). [3] The trailing edge control surface was a part of baseline wing with NACA6510 airfoil at the root and NACA0010 at the tip of the wing having a pre-twist of approximately 5 [degree] along its span. Figure 1 shows the baseline wing with attached control surface.

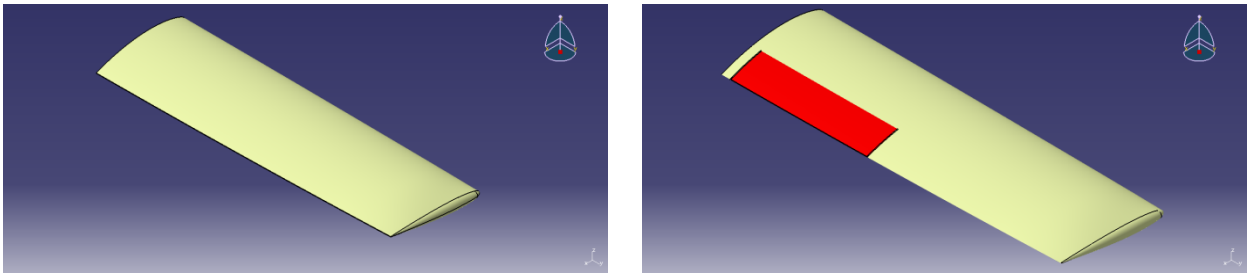

Figure 1. Baseline Wing Geometry (Left) and Control Surface (shown in red) Attached to the Baseline Wing Geometry (Right)

Designed hybrid control surface consists of two parts. The first part is made of a compliant material and attached to the main wing, whereas the second part is made of a composite material and forms the trailing edge of the wing. Figure 2 shows hybrid trailing edge control surface.

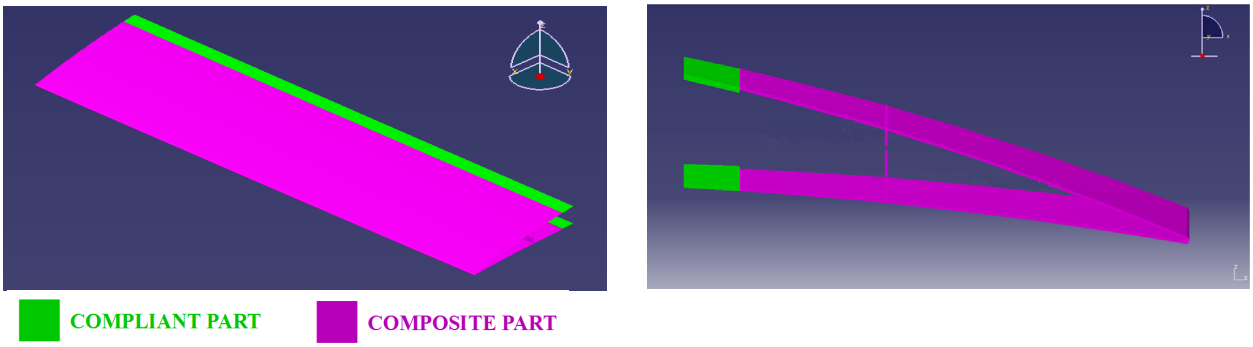

Figure 2. The Hybrid Trailing Edge Control Surface – Isometric View (Left) and Side View (Right)

The composite part of the hybrid trailing edge control surface has 1.08 [mm] thickness based on the previous studies of similar UAV designs [4] while the compliant part of the control surface is 2 [mm] thick. In comparison to the compliant material which undergoes significant deformations, the composite part of the control surface shows almost a rigid body motion. By deforming upper compliant part more than lower one by means of servo motors, downward deflection of the control surface is achieved. Since it is easier to deform the compliant flexible part to obtain the required control surface position (i.e. the position of the trailing edge), it was expected that the required servo motor forces would be small. Moreover, the use of this hybrid control surface concept leads to a close profile of the control surface at

the trailing edge in contrary to previous studies in which an unconventional aluminum open trailing edge control surface was designed [4].

2. STRUCTURAL ANALYSIS

The solid model of the hybrid trailing edge control surface was modeled by using CATIA V5-6R2012 package program for FEA along with moment arms of servo motors and actuations rods. Servo motor forces were transmitted to the hybrid control surface by means of transmission parts shown in Figure 3.

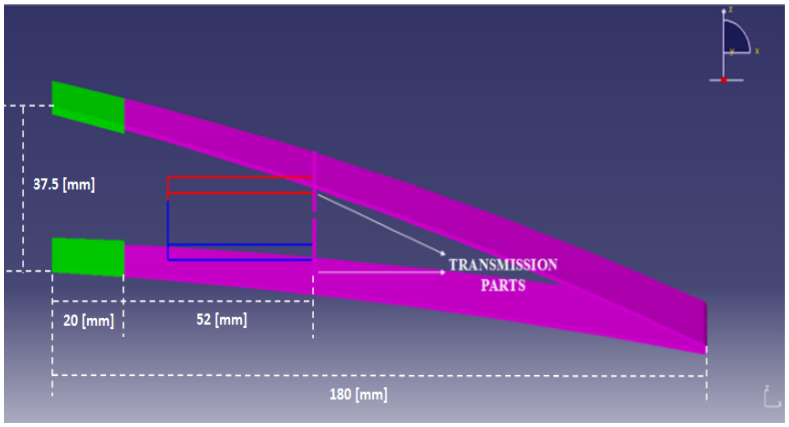

Figure 3. Transmission Parts of the Control Surface - The Servo Motors to Actuate the Upper Surface shown in Red; the Servo Motors to Actuate the Lower Surface shown in Blue

As it can be seen from Figure 3, red moment arms and actuation rods transmit the servo motor forces to the upper surface of the control surface while blue moment arms and actuation rods transmit to the lower surface of the control surface.

Upon generating the solid model of the control surface by using CATIA V5-6R2012, the model was imported into Static Structural module of ANSYS Workbench v14.0 for FEA. Actuation rods and moment arms were modeled as beams having circular cross section with 1.25 [mm] radius. Figure 4 shows the servo actuation rods and moment arms as lines.

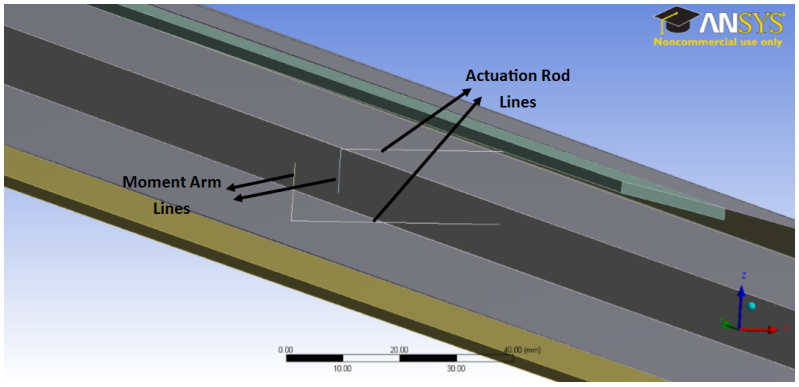

Figure 4. Servo Actuation Rods and Moment Arms Modeled as Lines

In the analyses, the composite part, which is 7781 E-Glass Fabric – Araldite LY5052 Resin – Aradur HY5052 Hardener Laminated, was modeled as a linear isotropic elastic material instead of an orthotropic one. Neoprene rubber, which is a hyperelastic material used for compliant skin, was imported from the

material library of the ANSYS Workbench v14.0. The density of the neoprene rubber was assigned as 1250 [kg/m^3]. [5] The moment arms and actuation rods were modelled as structural steel. Table 1 shows the properties of the materials used in FEA of the hybrid trailing edge control surface. Figure 5 shows the nonlinear stress-strain curves of uniaxial, biaxial and shear test data of neoprene rubber.

Table 1 Properties of the Materials used in the FEA of the Hybrid Trailing Edge Control Surface

Material	Young's Modulus	Poisson's Ratio	Density
Composite	70 [GPa]	0.3	1513 [kg/m^3]
Structural Steel	200	0.3	7850 [kg/m^3]

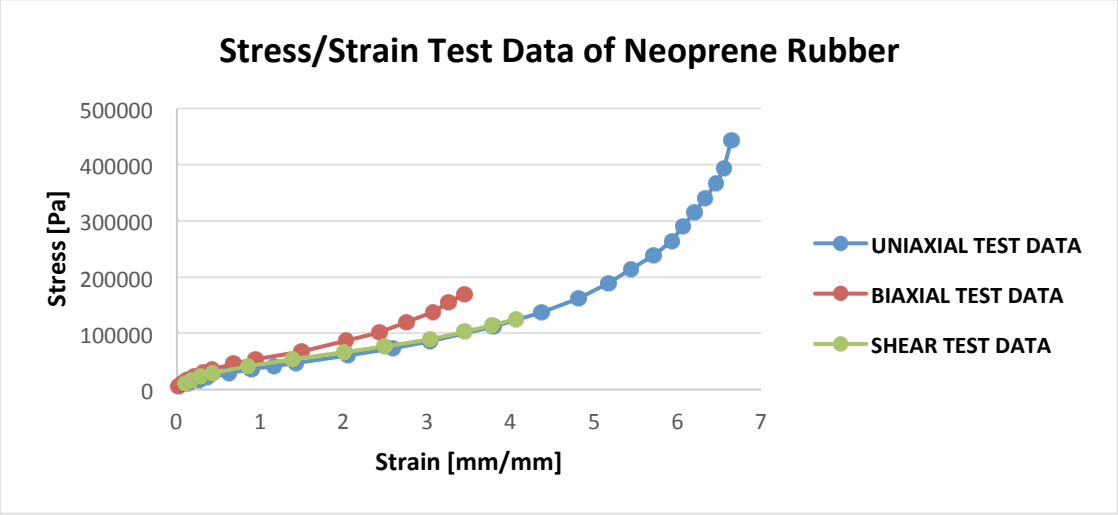

Figure 5. Stress/Strain Test Data of Neoprene Rubber

A perfect bond between the neoprene rubber part and the composite part was assumed. Since only the control surface of the wing was studied, wing and rear spar were not modeled and assumed to provide a rigid support to the compliant part. Therefore, the edges of the neoprene rubber part which connects the control surface to the rear spar was fixed for all degrees of freedoms. In the FEA, servo motors were assumed to be rigid and not modeled. One side of the moment arm was attached to the servo motor and the other side of it was attached to the actuation rod. At the end of the moment arm that is connected to the servo motor all displacement and rotation components are set to zero, except y-axis rotation. The connection between the transmission part and the actuation rods were assumed to be rigid. Figure 6 shows the fixed surfaces of the neoprene rubber part of the control surface.

After boundary conditions were defined, convergence studies were performed in order to decide element sizes of composite and compliant parts of the control surface. Figure 7 shows convergence studies for composite part with 20, 30, 40, 50 [mm] element sizes and neoprene rubber part 5, 10, 15, 20 and 25 [mm] element sizes. According to the convergence studies, composite part was modeled with 4-noded quadrilateral shell elements with element size of 30 [mm] and compliant part was modeled with 20-node brick elements with 10 [mm] edge size.

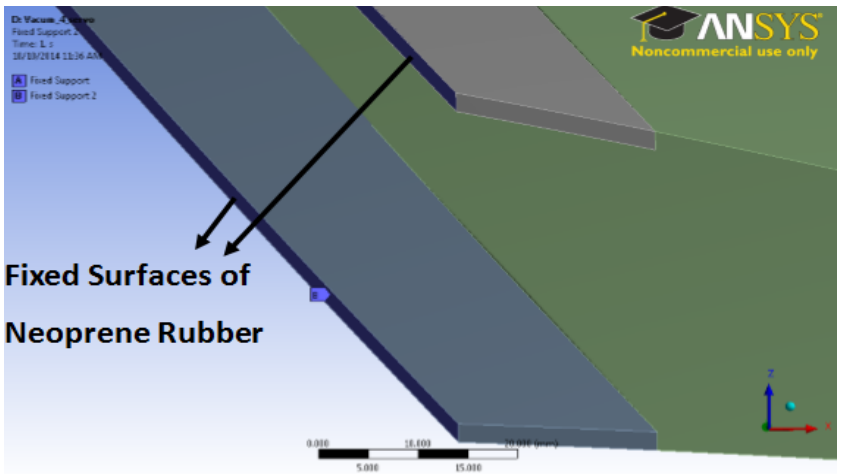

Figure 6. Fixed Surfaces of the Neoprene Rubber Part of the Control Surface

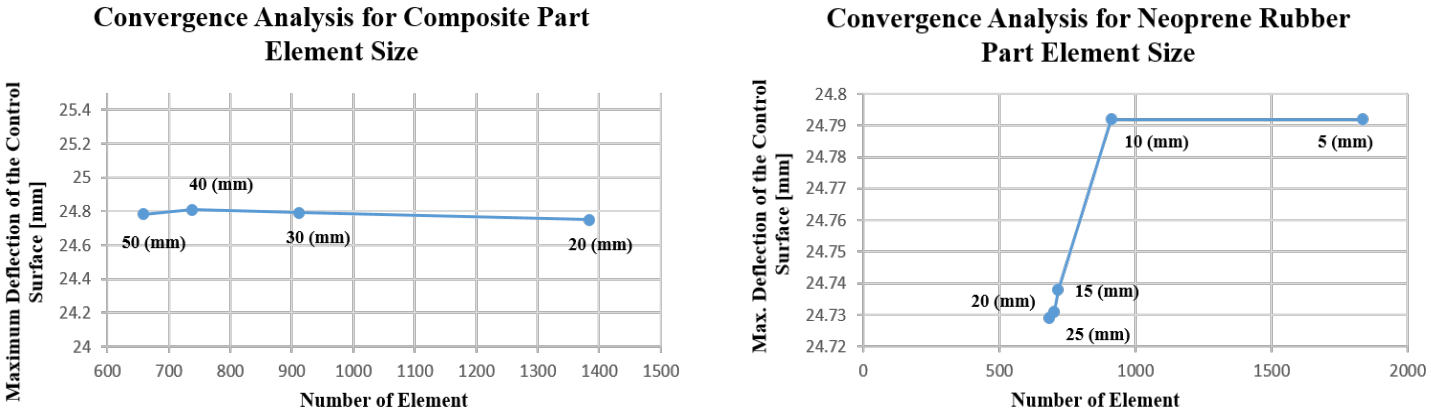

Figure 7. Convergence Analyses - for Composite Part (Left) and for Neoprene Rubber Part (Right)

The connection between the moment arms and the actuation rods was modeled like a pin joint, that is, except for rotation about one particular axis, all degrees of freedom are the same for both parts. To model this joint, coincident nodes of the moment arm and the actuation rod were coupled in x, y and z displacements, and rotations about x and z-axes. Only rotation about y-axis was not coupled, indicating that moment arms and actuation rods can rotate about y-axis independently, see Figure 8.

2.1 Structural Analysis in-Vacuo

In this part, FEA of the model explained in the previous section were conducted under standard earth gravity loading. During this study, the number and location of the servos were changed. For the effective camber increase of the control surface, 25 [mm] downward deflection of the trailing edge was aimed. For that purpose, four, five and six servo motors configurations were structurally analyzed and optimized in terms of weight and desired shape of the control surface.

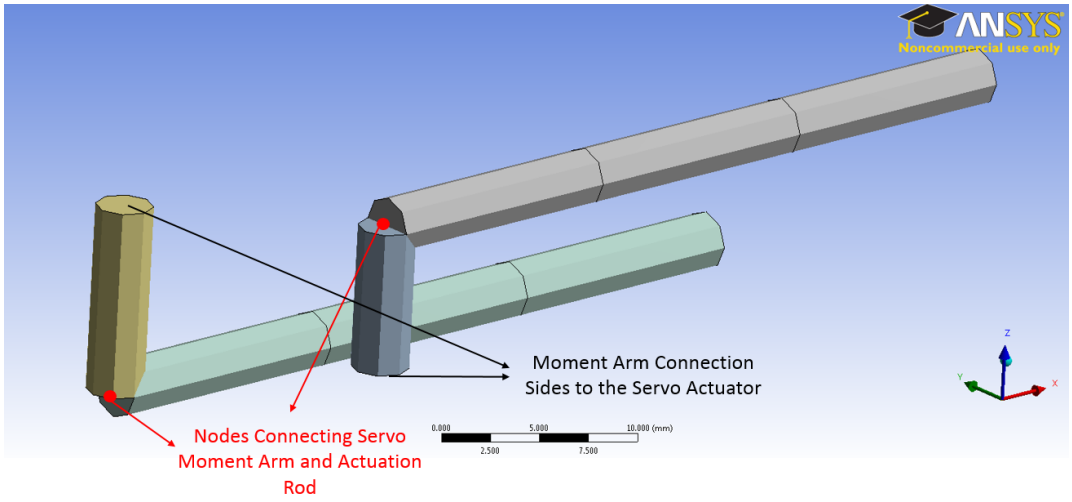

Figure 8. Coupled Nodes of Moment Arm and Actuation Rods and Moment Arm Connection Sides to the Servo Motors

In four servo motors configuration, the upper control surface is actuated by two servo motors and the lower control surface is actuated by two servo motors. In five servo motors configuration, on the other hand, three servo motors are used to actuate the upper part and two servos motors are used to actuate the lower part. Finally, in six servo motors configuration, the upper control surface is actuated by three servo motors and the lower control surface is actuated by three servo motors. In Figure 9 the locations of the servo motors to actuate the upper surface and the lower surface are shown in red and blue, respectively. In Figure 9,

- RU represents the servo motor close to root of the wing and actuates the upper control surface.
- RL represents the servo motor close to root of the wing and actuates the lower control surface.
- TU symbolizes the servo motor close to tip of the wing and actuates the upper control surface.
- TL symbolizes the servo motor close to tip of the wing and actuates the lower control surface.
- MU represents the middle servo motor that actuates the upper part of the control surface.
- ML represents the middle servo motor that actuates the lower part of the control surface.

In the FEA, for a 25 [mm] downward deflection of the trailing edge, the moment arm rotation about y axis was specified as 25 [degree] for the servo motors that actuate the upper surface and -5 [degree] for the servo motors that actuate the lower surface. Figure 10, Figure 11 and Figure 12 show the transverse displacements (Z direction) of the control surface according to conducted analysis for four, five and six servo motors configurations design, respectively.

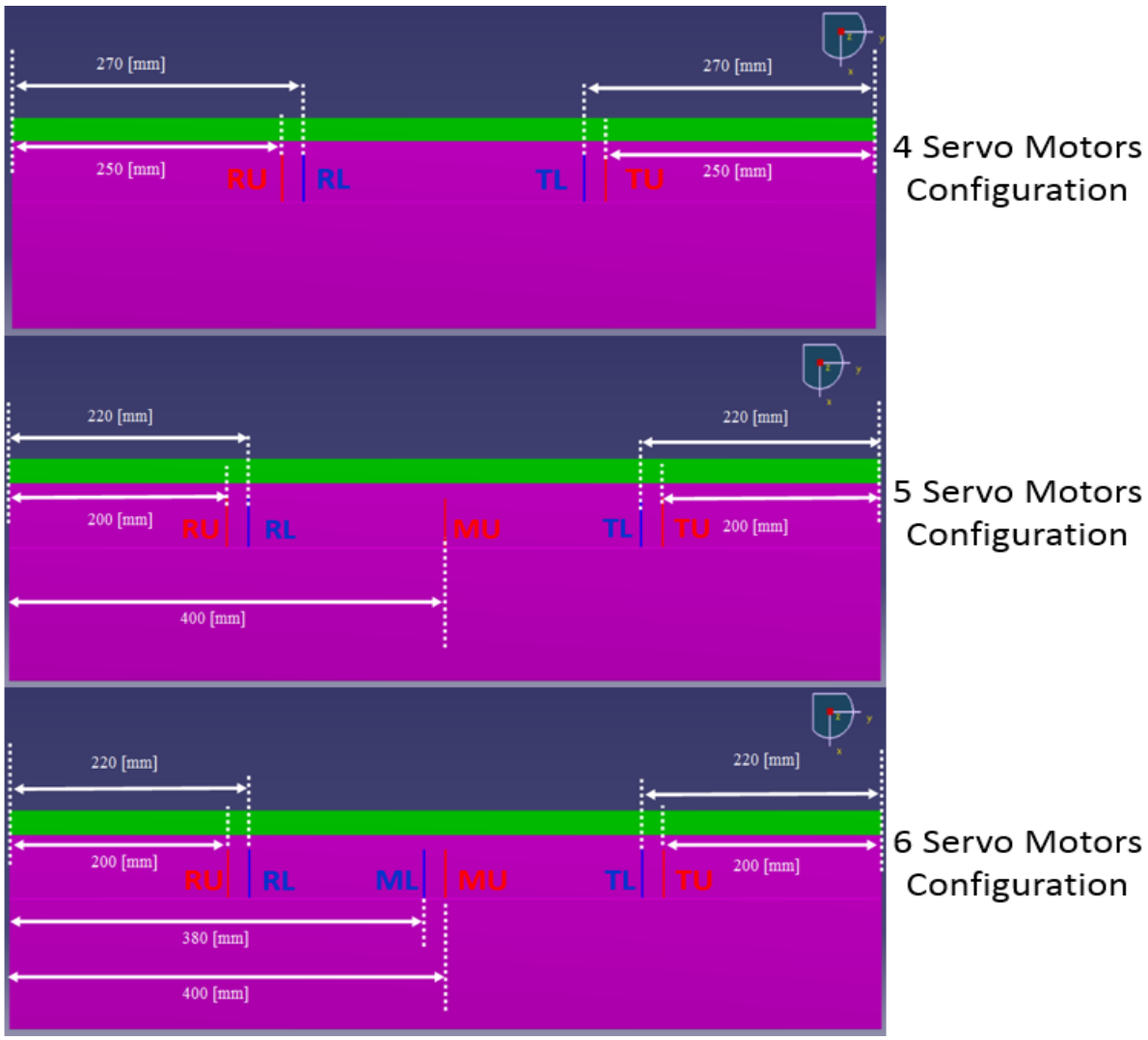

Figure 9. Locations of the Servo Motors. The Servo Motors that actuate the Upper Surface are shown in Red and the Lower Surface are shown in Blue

2.2 Comparison of the Four, Five and Six Servo Motors Configurations

In this part, according to results from analyses, four, five and six servo motors configurations were compared in terms of moment reactions of each servo motors, desired shape of the control surface and weight. As it can be seen from Figure 10, Figure 11 and Figure 12 all of the servo motor configurations provide the desired shape of the control surface. Moreover, it is known that the less the number of the servos is the better to achieve lower weight. In addition, as moment reaction occurred on the servo motor increases, the need for a bigger servo motor increases. Therefore, the less moment reaction on each servo motor is better in terms of weight and dimensions of the servos. Due to limited space in the control surface, it is preferred to use small servo motors in the design. Table 2 shows the moment reaction occurred on each servo motors for four, five and six servo motors configurations.

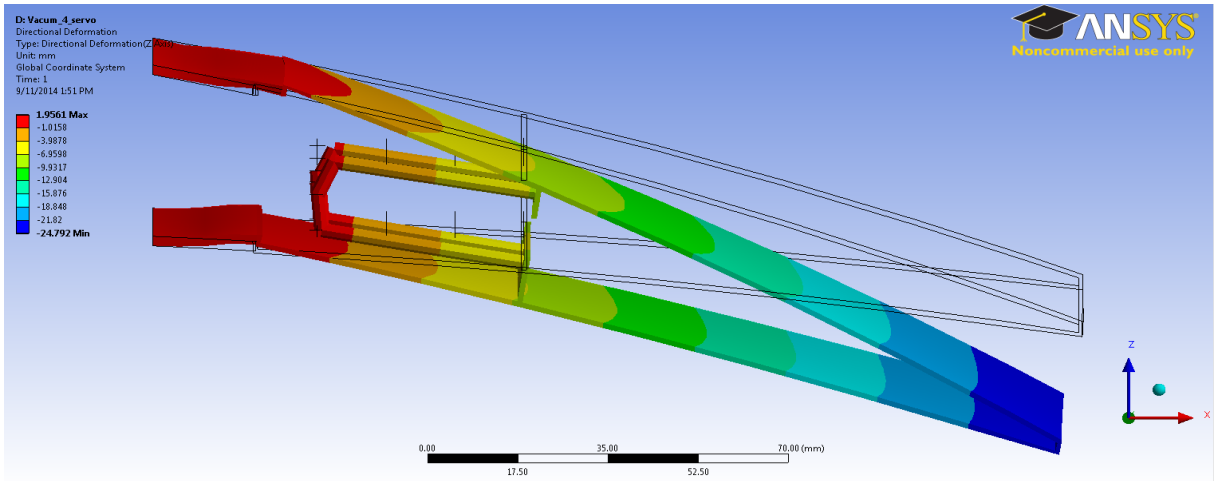

Figure 10. Transverse Displacement (Z Direction) of the Control Surface in Four Servo Motors Configuration Design - (max. 24.792 [mm])

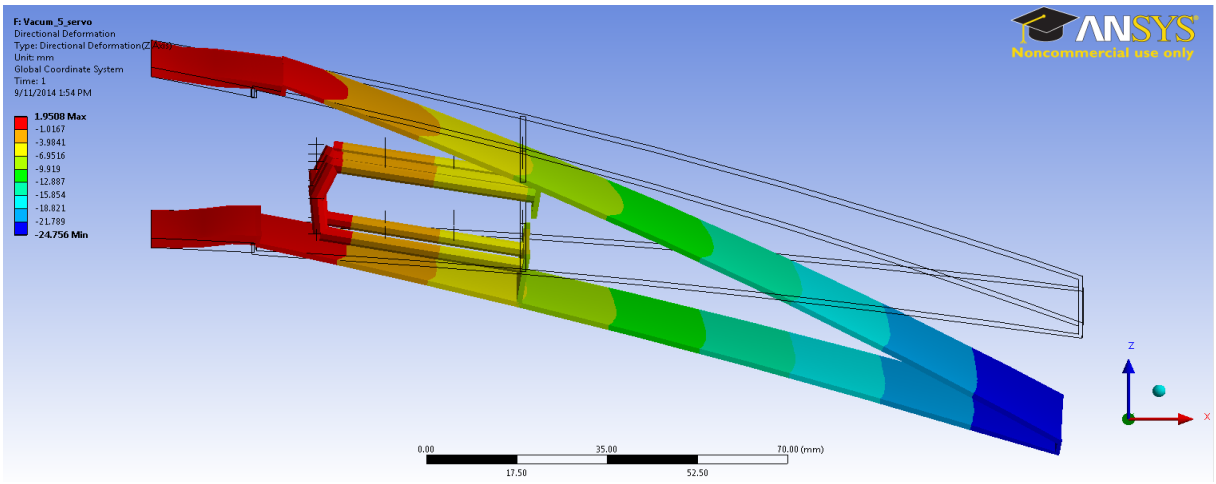

Figure 11. Transverse Displacement (Z Direction) of the Control Surface in Five Servo Motors Configuration Design - (max. 24.756 [mm])

As it can be seen from Table 2, highest moment reactions occur in four servo motors configuration for each servo motor. Least moment reactions on each servo motor are obtained in five servo motors configuration. In Table 2, smallest moment reaction occurred on the each servo motor for the each location is given as bold and underlined. Moreover, in six servo motors configuration, negative moment reaction appears on the servo motor which is in the middle of the control surface, to actuate the lower control surface. This shows the redundancy of the middle servo motor of the lower control surface. Taking into consideration of these results it is decided to use five servo motors configuration in the design of the control surface.

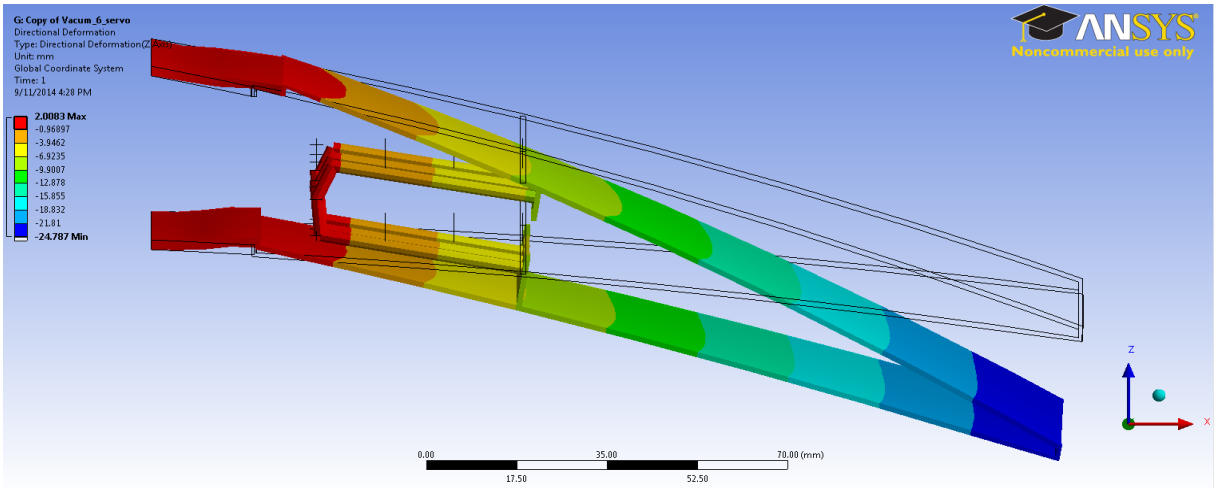

Figure 12. Transverse Displacement (Z Direction) of the Control Surface in Six Servo Motors Configuration Design - (max. 24.787 [mm])

Table 2 Moment Reactions Occurred on the Servo Motors for Four, Five and Six Servo Motors Configurations

	Four Servo Motors Configuration	Five Servo Motors Configuration	Six Servo Motors Configuration
Servo Motors	**Moment Reactions [kg-cm]**	**Moment Reactions [kg-cm]**	**Moment Reactions [kg-cm]**
RU	1.88	**1.34**	1.37
MU	-	1.12	**1.05**
TU	1.99	**1.46**	1.48
RL	1.48	**0.5**	0.85
ML	-	-	-0.62
TL	**0.76**	0.79	1.03

2.3 Structural Analysis under Aerodynamic Loads

After deciding to use five servo motors configuration from the structural analyses in-Vacuo condition, the pressure data of landing phase of the flight provided by the similar study was imported to the control surface by using interpolation method [1]. Figure 13 shows the pressure distribution applied to the structure. By using the imported pressure data, FEA was repeated for five servo motors configuration with same boundary conditions and loadings except the moment arm rotation about y-axis for the servo motors that actuate the upper surface of the control surface. In the FEA under the aerodynamic loading, in order to achieve 25 [mm] downward deflection of the trailing edge, the moment arm rotation about y-axis was specified as 25.7 [degree] for the servo motors that actuate the upper surface. Figure 14 shows the transverse displacement of the control surface under the aerodynamic loads.

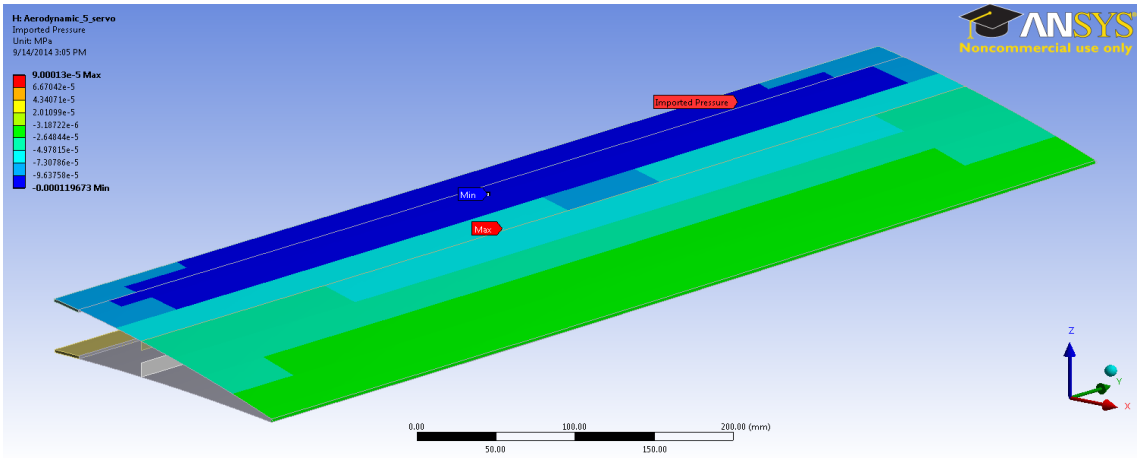

Figure 13. Imported Pressure to the Control Surface – Max. 0.9 [MPa]

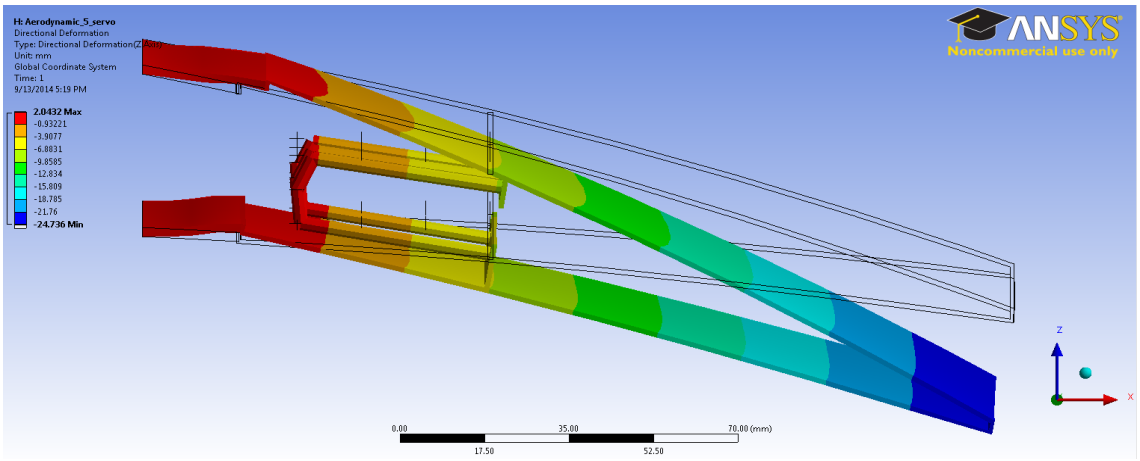

Figure 14. Transverse Displacement (Z Direction) of the Control Surface in 5 Servo Motors Configuration Design under the Aerodynamic Load- (max. 24.736 [mm])

Table 3 shows the maximum values of von-Mises strain and stress distribution and beam stress (combination of axial and bending stresses, which is called as combined stress) distribution in actuation rods and moment arms.

Table 3 Maximum Values for the von-Mises Strain and Stress and Stress Distribution in Actuation Rods and Moment Arms

	Maximum Values of the Analysis Results
von-Mises Strain	0.32
von-Mises Stress	10.29 [MPa]
Maximum Combined Stress in Actuation Rods and Moment Arm	62.459 [MPa]

According to results of the analyses shown in Table 3, maximum strain value, which is 32%, occurs at neoprene rubber part at the upper surface of the control surface. According to Figure 5, neoprene rubber is safe in this condition. As expected, in the composite part, strain values are extremely small. Therefore, the composite part makes almost a rigid body motion. The maximum stress occurs in the transmission part, which is made of composite. It can be seen from Table 3, maximum stress value is 10.29 [MPa] and this value is significantly lower than the ultimate tensile strength (369 [MPa]) of the composite used [6]. Thus,

the composite part is also in the safe region. The maximum stress occurred in actuation rods and moment arms is 62.459 [MPa] and this value is lower than the tensile yield strength of structural steel that is the material of the actuation rods and moment arms [7]. Hence, these parts are in the safe region as well.

3. SERVO MOTOR SELECTION AND PLACING

Table 4 shows the moment reactions results of the design with five servo motors for each servo motor under aerodynamic loading. In order to select servo motors, these moment reaction values were multiplied by safety factor of 1.5, which are also shown in Table 4. Maximum torque values among the servo motors for actuating the upper part and lower part of the control surface are given bold and underlined.

Table 4 Moment Reactions Occurred on the Servo Motors for Five Servo Motors Configuration and Moment Reactions after Applying a Safety Factor of 1.5

Servo Motors	Moment Reactions [kg-cm]	After applying a Safety Factor of 1.5 [kg-cm]
RU	1.42	2.13
MU	1.7	**2.55**
TU	1.54	2.31
RL	0.97	1.46
TL	1.26	**1.89**

It can be seen from Table 4, the highest torque value among the servo motors for the actuation of upper surface is about 2.55 [kg-cm] and for the actuation of lower surface is about 1.89 [kg-cm]. According to these values, servo motors were selected separately for upper and lower surface actuation. Table 5 shows the properties of selected servos.

Table 5 Properties of Servos to Actuate the Upper Part and Lower Part of the Control Surface

	Servo to Actuate the Upper Part	Servo to Actuate the Lower Part
Torque at 6 [V]	2.5 [kg-cm]	2 [kg-cm]
Dimensions	29 x 13 x 30 [mm]	23 x 12 x 30 [mm]
Weight	19 [gr]	9.3 [gr]

Finally, the selected servo motors and actuation rods were implemented to the designed assembly by using CATIA V5-6R2012 package software. Figure 15 shows the spacing of servo motors in five servo motors configuration.

4. CONCLUSION

This study presents the design and analysis of a new unconventional hybrid trailing edge control surface of an UAV. Three configurations which have different number of servo motors were compared particularly by considering weight and torque optimization. Configuration with five servo motors was selected to be used after comparisons in-Vacuo condition. Then, selected control surface design was structurally analyzed under the aerodynamic loads. Finally, servo motors were placed into the control surface and it was shown that selected design is realizable.

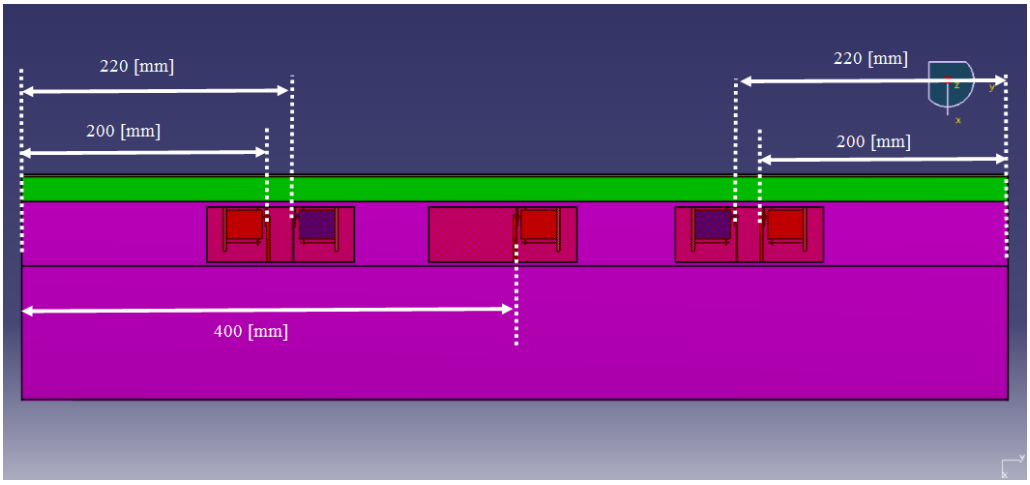

Figure 15. Spacing of the Servo Motors in Five Servo Motors Configuration

ACKNOWLEDGMENTS

The work presented herein has been partially funded by the European Community's Seventh Framework Programme (FP7) under the Grant Agreement 314139. The CHANGE project ("Combined morphing assessment software using flight envelope data and mission based morphing prototype wing development") is a L1 project funded under the topic AAT.2012.1.1-2 involving nine partners. The project started in August, 1, 2012.

İlhan Ozan Tunçöz and Yosheph Yang thank to TUBITAK (The Scientific and Technological Research Council of Turkey) for supporting them during their graduate education.

REFERENCES

1. Arslan, P., Kalkan, U., Tuncoz, İ.O., Tıraş, H., Yang, Y., Gürses, E., Şahin, M., Özgen, S., Yaman, Y., "Design of a Hybrid Trailing Edge Control Surface", *submitted to Journal of Intelligent Materials Systems and Structures.*
2. CHANGE FP7 Project, http://change.tekever.com/, *accessed on 10.09.2014.*
3. Aircraft Research Association (ARA), http://ara.co.uk/
4. TUBITAK Project 107M103, 2011, http://ae.metu.edu.tr/~yyaman/LabCapabilities/TUBITAK_107M103.pdf 2011, *accessed on 11/08/2014*
5. Cambridge University Engineering Department, *"Materials Data Book", 2003, pp. 10* http://www-mdp.eng.cam.ac.uk/web/library/enginfo/cueddatabooks/materials.pdf, *accessed on 24/02/2014*
6. Unlusoy, L.,"Structural Design And Analysis Of The Mission Adaptive Wings Of An Unmanned Aerial Vehicle", *Middle East Technical University, M. Sc. Thesis*, pp.14.
7. ANSYS v14.0 Workbench Help